



Supported Al–Ti bimetallic catalysts for 1-decene oligomerization: Activity, stability and deactivation mechanism



Hui Sun^{a,*}, Benxian Shen^a, Di Wu^b, Xiaofeng Guo^c, Deng Li^a

^aState Key Laboratory of Chemical Engineering, East China University of Science and Technology, Shanghai 200237, China

^bPeter A. Rock Thermochemistry Laboratory and NEAT ORU, University of California, Davis, CA 95616, United States

^cEarth and Environmental Sciences Division, Los Alamos National Laboratory, Los Alamos, NM 87545, United States

ARTICLE INFO

Article history:

Received 4 January 2016

Revised 17 March 2016

Accepted 19 March 2016

Available online 26 April 2016

Keywords:

Al–Ti bimetallic catalysts

1-Decene oligomerization

Activity

Stability

Deactivation mechanism

ABSTRACT

A variety of supported bimetallic catalysts were prepared through immobilization of AlCl_3 and TiCl_4 on different porous materials and used for the oligomerization of 1-decene in a fixed-bed reactor. The supported catalysts were characterized by various techniques including X-ray photoelectron spectroscopy (XPS), ^{27}Al MAS NMR, N_2 adsorption, adsorbed pyridine infrared (Py-IR), thermogravimetry and differential scanning calorimetry (TG–DSC), energy-dispersive spectrometry (EDS), and content measurement of active species. Their catalytic activity was examined and the underlying deactivation mechanism was explored. The initial catalytic activity was observed to be a linear function of the chlorine content of the supported catalyst. A catalyst using a coal-derived activated carbon support has the highest loading and exhibits the highest yield of polyalphaolefin (PAO), while a $\gamma\text{-Al}_2\text{O}_3$ -supported catalyst gives higher stability. In addition, thermal treatment of the $\gamma\text{-Al}_2\text{O}_3$ -supported catalyst results in reduced initial activity but enhanced stability. Both the loss of active species and the blockage and coverage of the pore structure by oligomers account for the deactivation of the supported catalyst.

© 2016 Elsevier Inc. All rights reserved.

1. Introduction

With a variety of excellent performance features including good thermal and oxidative stability, high viscosity index, good low-temperature fluidity, low volatility, low corrosiveness, and high biodegradability, synthetic lubricants find increasingly wide applications under extreme conditions [1–4]. Polyalphaolefin (PAO)-based synthetic lubricants are proven to offer high mechanical efficiency, low energy consumption, long equipment life, and comparative environmental benefits, and therefore have been attracting enhanced interest in both academic and industrial research [5–7].

Synthetic PAO base stocks are composed of branched alkanes with defined molecular weights. In general, they are manufactured from the cationically catalytic oligomerization of linear alpha-olefins with carbon numbers C6–C20 followed by hydrogenation. 1-Decene is the most commonly used starting alpha-olefin. Additionally, various catalysts such as homogeneous Lewis acid catalysts (e.g., AlCl_3 , BF_3) [3], transition metal complexes [8–11], reduced chromium [12–14], Ziegler–Natta catalysts [15], metal-olene catalysts [16–18], and different kinds of solid acid catalysts

[19–21] (including a variety of synthetic zeolites [22,23], ion exchange resins [24,25], and metal oxides [26]) are involved in the oligomerization reactions of alpha-olefins. Metal complexes are one type of commonly used catalysts because of their high activity and ability to achieve well-controlled molecular weight and stereochemistry of oligomers. However, their highly corrosive and hazardous features and disposal problem lead to researchers' incessant attempts to devise green processes in order to circumvent such drawbacks. Anchoring homogeneous complexes on various supports is considered a very promising method for minimizing the costs and environmental impact of metal complexes [27–29]. Extensive investigations on loading of active species are being carried out to screen supports and immobilization conditions. Moreover, although the deactivation of the resulting catalysts is realized to be a fundamentally important issue for optimizing performances and applications, it has not been understood very well, and the underlying mechanism is not clear.

In this work, we performed the catalytic oligomerization of 1-decene on supported Al–Ti bimetallic catalysts in a fixed-bed reactor. Catalysts were prepared by immobilization of AlCl_3 and TiCl_4 on a variety of porous supports. This study presents a quantitative relationship between the catalytic activity and chlorine content of supported catalysts and provides insight into the deactivation mechanism of supported Al–Ti bimetallic catalysts.

* Corresponding author.

E-mail address: sunhui@ecust.edu.cn (H. Sun).

2. Experimental

2.1. Materials

1-Decene (Dowpol Chemical International Corporation, China) is of >96.2% purity. Titanium tetrachloride, anhydrous ethanol, and diethyl ether (Shanghai Lingfeng Chemical Reagent Co., Ltd., China) and aluminum trichloride, benzene, toluene, acetone, and nitric acid (Sinopharm Chemical Reagent Co., Ltd., China) are analytical grade. All chemicals were used as obtained. However, if the reagents have been uncovered for a long time, they should be purified with dehydration and deoxygenation reagents prior to being used again in order to prevent water contamination. Coal-derived activated carbon (CDAC) (Shanghai Activated Carbon Co., Ltd., China), coconut shell activated carbon (CSAC) (Shanghai Xinhui Activated Carbon Co., Ltd., China), γ -Al₂O₃-1 and silica gel (Sinopharm Chemical Reagent Co., Ltd., China), γ -Al₂O₃-2 (China Research Institute of Daily Chemical Industry, China), and zeolites HZSM-5-1 (Si/Al = 50) and HZSM-5-2 (Si/Al = 360) (the Catalyst Plant of Nankai University, China) were employed as supports.

2.2. Preparation of immobilized AlCl₃-TiCl₄ catalysts

Catalysts were prepared by loading the active species AlCl₃ and TiCl₄ onto various supports including γ -Al₂O₃-1, γ -Al₂O₃-2, CDAC, CSAC, silica gel, and zeolites HZSM-5-1 and HZSM-5-2. The corresponding supported catalysts were labeled A1, A2, C1, C2, S, Z1, and Z2 (see Table 1). Various organic solvents including benzene, toluene, ethanol, diethyl ether, acetone, and carbon tetrachloride were used during the immobilization procedure.

At first, all as-received porous materials were pretreated to obtain different supports. Specifically, γ -Al₂O₃-1, γ -Al₂O₃-2, zeolites HZSM-5-1 and HZSM-5-2, and silica gel were heated at 400 °C in a SXC-1.5/10 muffle furnace (Hangzhou Lantian Instrument Co., Ltd., China) for 4 h and then cooled to room temperature in a desiccator. Activated carbon supports CDAC and CSAC were treated in 1 M nitric acid aqueous solution at room temperature for 8 h and then thoroughly washed with deionized water until the washing water reached neutral pH. After that, the resulting

supports were air-dried overnight at 110 °C and then conserved in the desiccator. Subsequently, active components AlCl₃ and TiCl₄ were immobilized onto different supports using a reflux apparatus under dry N₂. The quantities 16 g of AlCl₃ and 4.5 g of TiCl₄ were dissolved in 150 mL solvent. The molar ratio $n(\text{Al})/n(\text{Ti})$ and the mass ratio of AlCl₃ to support were fixed at 5 and 0.4 for every immobilization. The solution was transferred into a 250 mL flask containing 40 g support under high-purity nitrogen flow (80 mL min⁻¹), followed by heating of the mixture at the desired temperature for 12 h with a magnetic stirrer. The as-prepared fresh catalyst slurry with solvent was divided into two parts. A small part of it was heated in a glass tube under N₂ flow (80 °C) for the removal of the solvent. The solvent-free sample was kept in a desiccator for further characterization. The rest was loaded into a fixed-bed reactor for the oligomerization reaction and then thoroughly swept (for at least 6 h) using hot N₂ flow (80 °C and 120 mL min⁻¹) in order to repel residual solvent in catalyst. The slurry containing solvent was used while filling the column in order to prevent the catalyst from being exposed to atmosphere.

A sample of catalyst using γ -Al₂O₃-1 support underwent special heating treatment at 400 °C in a muffle furnace under nitrogen flow (100 mL min⁻¹) for 4 h, labeled as A1-2 (see Table 1).

2.3. Oligomerization procedure

The oligomerization of 1-decene was performed in a custom-built fixed-bed reactor (Fig. 1) with an inner diameter of 15 mm. A plate formed of 10–20 mesh silica sand was fixed at the bottom of the reactor in order to hold the catalyst, and acted as flow distributor. The reactor was filled with around 60 mL catalyst and its temperature was raised to 80 °C under the high-purity nitrogen flow (120 mL min⁻¹). 1-Decene was introduced into the bottom of the reactor using a 2PB-00C plunger pump (Beijing Xingda Technology Development Corporation, China). Liquid hourly space velocity (LHSV) was fixed at 0.5 h⁻¹ for the oligomerization of 1-decene. The product mixture was separated through vacuum distillation. Only the >280 °C fraction was collected as the PAO product and used for further analyses.

Table 1
Supported catalysts using various supports or preparation conditions.

Catalyst	Support	Immobilization solvent	<i>t</i> (h) ^c	<i>T</i> ₁ (°C) ^d	<i>T</i> ₂ (°C) ^e
A1-1	γ -Al ₂ O ₃ -1	Carbon tetrachloride	12	80	No
A1-2	γ -Al ₂ O ₃ -1	Carbon tetrachloride	12	80	400
A2	γ -Al ₂ O ₃ -2	Carbon tetrachloride	12	80	No
C1-1	CDAC ^a	Benzene	12	80	No
C1-2	CDAC ^a	Toluene	12	80	No
C1-3	CDAC ^a	Ethanol	12	80	No
C1-4	CDAC ^a	Diethyl ether	12	80	No
C1-5	CDAC ^a	Acetone	12	80	No
C1-6	CDAC ^a	Carbon tetrachloride	12	80	No
C1-7	CDAC ^a	Carbon tetrachloride	6	80	No
C1-8	CDAC ^a	Carbon tetrachloride	8	80	No
C1-9	CDAC ^a	Carbon tetrachloride	10	80	No
C1-10	CDAC ^a	Carbon tetrachloride	24	80	No
C1-11	CDAC ^a	Carbon tetrachloride	36	80	No
C1-12	CDAC ^a	Carbon tetrachloride	12	50	No
C1-13	CDAC ^a	Carbon tetrachloride	12	60	No
C1-14	CDAC ^a	Carbon tetrachloride	12	70	No
C2	CSAC ^b	Carbon tetrachloride	12	80	No
S	Silica gel	Carbon tetrachloride	12	80	No
Z1	Zeolite HZSM-5-1	Carbon tetrachloride	12	80	No
Z2	Zeolite HZSM-5-2	Carbon tetrachloride	12	80	No

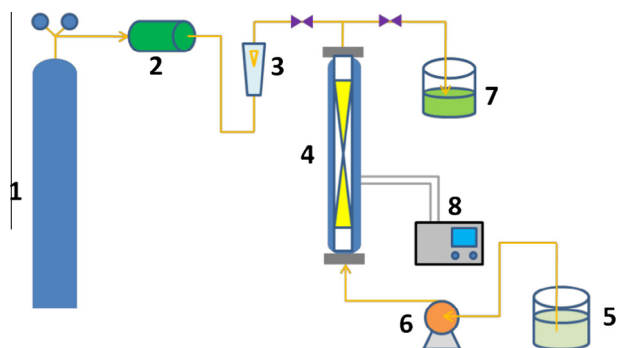
^a Coal-derived activated carbon.

^b Coconut shell activated carbon.

^c Immobilization time.

^d Immobilization temperature.

^e Heating treatment temperature.



1 - N₂ cylinder; 2 - dryer; 3 - flowmeter;
4 - fixed-bed reactor; 5 - raw material tank;
6 - pump; 7 - product tank; 8 - temperature controller.

Fig. 1. Flowchart for oligomerization.

2.4. Analysis and characterization

Kinematic viscosities of PAO products were measured using a SYD-265C capillary viscosity meter (Shanghai Geological Instrument Factory, China) according to ASTM D445. The viscosities of PAO were tested at 40 and 100 °C, denoted as ν_{40} and ν_{100} , respectively. The viscosity index (VI), which can reflect the temperature dependence of viscosity of the PAO product, can be derived from ν_{40} and ν_{100} according to ASTM D2270. The freezing point (FP) was measured on a SYP1022-2 freezing point analyzer (Shanghai Boli Instrument Co., Ltd., China).

Chlorine content of the catalysts was determined using a ZWC-2001 salt content analyzer (Jiangsu Jierui Instrument and Equipment Co., Ltd., China). First, a catalyst sample weighing around 1 g was treated with 40 mL 0.5 M nitric acid aqueous solution for 8 h and washed at least three times with deionized water. The solution was separated through centrifugation and collected. The treating solution for each catalyst was diluted to 250 mL with deionized water. The mass fractions of chlorine in fresh and deactivated catalysts, x_{Cl} , could be simply calculated according to $x_{Cl} = 250c_0/m_0$, where c_0 is the chlorine content in solution, g mL⁻¹, and m_0 is the mass of the catalyst sample, g. In addition, chlorine content in synthetic PAO product was determined using a WK-2D microcoulometric analyzer (Jiangfen Electroanalytical Instrument Co., Ltd., China).

Morphologies of the catalyst samples were determined using a JSM-6360LV scanning electronic microscope (JEOL, Japan) at a scan voltage of 15 kV. Element point analysis and map scanning were carried out on a Falcon energy-dispersive spectrometer (EDS) (EDAX Inc., USA). Five to eight points were measured at various positions to obtain an average elemental composition.

The specific surface area and pore structure of the supports and catalysts were analyzed on an ASAP2010 micropore physisorption analyzer (Micromeritics Instrument Corporation, USA). Prior to nitrogen adsorption, all samples were heated at 190 °C for 6 h. The testing pressure ranged from 0.001 to 102.41 kPa.

Thermogravimetry and differential scanning calorimetry (TG–DSC) was conducted on a SDT Q600 system (TA instruments, USA). The catalyst sample was placed in a platinum crucible and heated from room temperature to 800 °C at 10 °C min⁻¹ under the oxygen flow (40 mL min⁻¹).

XPS spectra of the samples were collected using a PHI-5300 ESCA X-ray photoelectron spectroscopy system (PE, USA) equipped with a Mg anode (14 kV, 250 W).

Content for Al and Ti in product streams was determined using a 725-ES inductively coupled plasma optical emission spectrometer (ICP-OES) (Agilent Technologies, USA).

The magic angle spinning (MAS) ²⁷Al NMR spectra were recorded using an Avance III 400 MHz spectrometer (Bruker, Germany) operating at 78.2 MHz and spun at 5 kHz.

Adsorbed pyridine infrared (Py-IR) analyses were performed on a Tensor 27 FTIR spectrometer (Bruker, Germany). At first, the samples were evacuated in situ in an IR cell. Pyridine was adsorbed and then desorbed at 25 °C for 30 min and then at 150 °C for 60 min.

The yield of PAO product, Y , was defined as $Y = m_p/m_D \times 100\%$, where m_p and m_D are the mass of the >280 °C fraction in the synthesized mixture and the raw material 1-decene, respectively. Y is calculated according to collected product within the first 2 h time on stream to determine the catalytic performance of various freshly prepared catalysts. Meanwhile, a series of oligomerizations were performed continuously in the same fixed-bed reactor in order to evaluate the catalyst stability.

3. Results and discussion

3.1. Catalytic performance of AlCl₃–TiCl₄ on various supports

The nature and pore structure of the support can largely determine the immobilization of the active species and therefore can have an extremely significant effect on catalytic performance. In order to evaluate such influences, various porous materials including γ -Al₂O₃ with distinct pore size, different types of activated carbon, silica gel, and zeolites HZSM-5 with different Si/Al molar ratios were used as the supports in the preparation of immobilized catalysts. Their chlorine content, x_{Cl} , and yield of PAO, Y , are presented in Fig. 2a. In addition, the micropore analysis results for different supports are listed in Table 2. The chlorine content is found in the following order: CDAC > γ -Al₂O₃-1 > γ -Al₂O₃-2 > CSAC > HZSM-5-2 > HZSM-5-1 > silica gel. Overall, the yield of PAO ranks in almost the same order, except for CSAC and HZSM-5, which have reversed yields. This indicates that CDAC and γ -Al₂O₃ with small pore size are promising candidates for immobilization of AlCl₃–TiCl₄ involved in catalytic synthesis of PAO. In the case of CDAC, the highest x_{Cl} and the largest Y are observed as 14.2% and 90.81%, respectively. In contrast, silica gel has a low chlorine content (x_{Cl} equals 0.6%), although possessing relatively high specific surface area (730 m²/g; see Table 2); hence, it fails to catalyze the oligomerization of 1-decene efficiently (with Y of only 3.10%). Taking all the supports used here into consideration, it seems that there is no strong dependence of x_{Cl} on the specific surface area. It has been proven that γ -Al₂O₃ can be an excellent medium for binding AlCl₃, owing to its inherently abundant OH groups, which have a strong bonding affinity for the active species [30]. The present results support this conclusion by providing both γ -Al₂O₃-supported catalysts with around 88% PAO yield.

The formation and distribution of Al and Ti on the surfaces of various supports are revealed by XPS, ²⁷Al MAS NMR, and SEM/EDS mapping analyses (Fig. 3). In Fig. 3a, all samples display the Al2p_{1/2} (74 eV) and Ti2p_{1/2} (465 eV) and Ti2p_{3/2} (460 eV) doublet, associated with the binding energy of the oxygenated states of Al and Ti, respectively. Catalyst S displays a bonding energy of 73 eV, corresponding to Al2p_{3/2}. The ²⁷Al MAS NMR results (Fig. 3c) indicate that AlCl₃ species can be 4-, 5-, and 6-coordinated by binding oxygen groups from the support surface, which agrees with previous studies [31–33]. From SEM/EDS mapping analysis (Fig. 3d), the Al and Ti species are found to be highly dispersed on the surface of the support. Using oxygen as a reference, the relative values of the molar ratio Ti/O for different samples, therefore, can be estimated from their corresponding XPS peaks in order to evaluate the relative content of active species on catalyst surface. In Fig. 3b, Ti/O presents an order generally consistent with the chlorine content for various supports. Among all the fresh catalyst

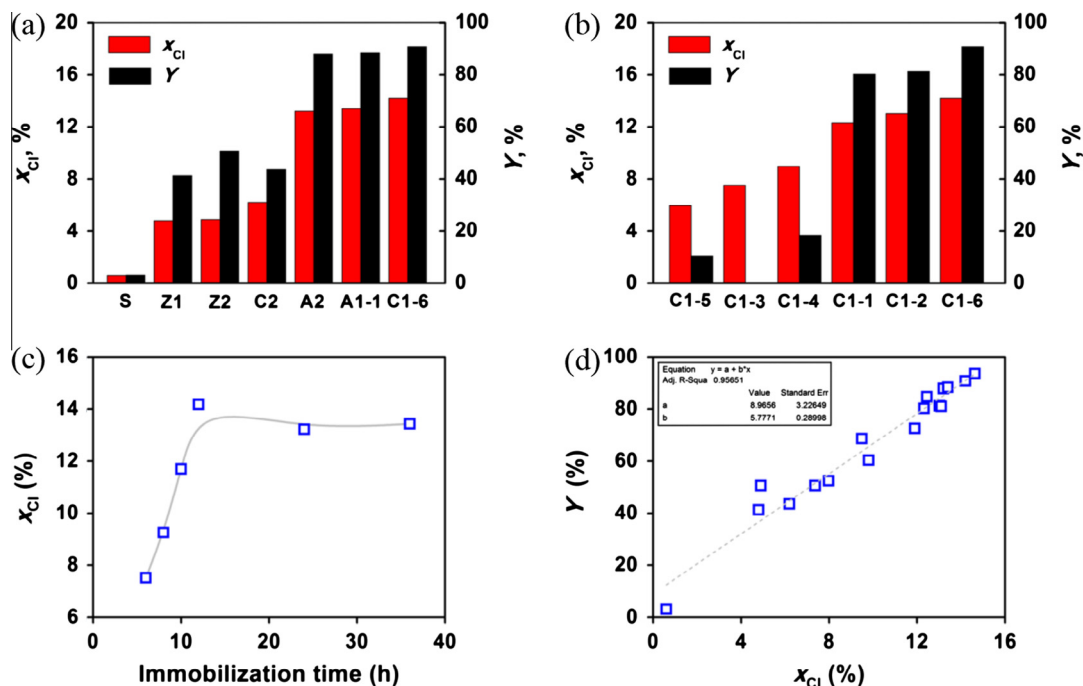


Fig. 2. Chlorine content (x_{Cl}) and PAO yield (Y) of catalysts (a) using different supports, (b) using different immobilization solvents, and (c) at different immobilization times; (d) relationship of chlorine content (x_{Cl}) to PAO yield (Y).

Table 2
BET specific surface area, pore volume, and average pore diameter of various supports.

Support	S_{BET} (m^2/g) ^a	V_p (cm^3/g) ^b	d_p (nm) ^c
γ - Al_2O_3 -1	281.38	0.4396	6.25
γ - Al_2O_3 -2	164.83	0.8036	19.52
CDAC	820.33	0.4144	2.24
CSAC	718.44	0.4026	2.02
Silica gel	730.04	0.4737	2.59
HZSM-5-1	308.30	0.2536	3.29
HZSM-5-2	321.84	0.3105	3.81

^a Specific surface area.

^b Pore volume.

^c Average pore diameter (1.7–300 nm).

samples, C1-6 has the highest value, while S has the lowest one. As compared with the sample A1-1, sample A1-2 (with heating treatment at 400 °C) has lower Ti/O due to the escape of active species from the support during heating. Next, the acidity of samples was characterized by Py-IR analysis. A characteristic band with respect to coordination of pyridine molecules to Lewis acid sites can be clearly identified at $\sim 1450\text{ cm}^{-1}$ for all tested samples (Fig. 3e). However, almost no pyridinium ions can be detected (note the absence of the $\sim 1540\text{ cm}^{-1}$ band), suggesting that the catalysts have no Brønsted acidity. Again, sample A1-2 shows fewer Lewis acidic sites than A1-1 resulting from the impact of thermal treatment on A1-2.

A previous study indicated that supported catalysts have increasing catalytic activity and stability with increasing average pore size of γ - Al_2O_3 supports because of less pore blockage and less diffusion resistance of oligomer molecules within larger pores of the catalysts [34]. However, this conclusion cannot be drawn from our results. Instead, the catalysts using two γ - Al_2O_3 supports possessing different average pore diameters (6.25 nm for γ - Al_2O_3 -1 and 19.52 nm for γ - Al_2O_3 -2) seem to display comparable catalytic activity (PAO yields of 88.4% vs. 87.9%). A reasonable explanation is that the accessible acidic sites are highly dispersed on the surfaces of supports and therefore contribute equally to the catalytic

activity. This can be supported by our characterizations presented above. From XPS analysis, similar content of active species is found on the surfaces of both catalysts.

3.2. Effect of immobilization solvents

During the immobilization process, the solvent can play a critical role in impregnating active species into a porous support and endowing a catalyst with high catalytic activity [32,35]. Various solvents including benzene, toluene, ethanol, diethyl ether, acetone, and carbon tetrachloride were used for immobilization of $AlCl_3$ and $TiCl_4$ on CDAC support. Both x_{Cl} and Y are observed to be fairly distinct for various supports (Fig. 2b). Catalyst C1-6 (using carbon tetrachloride) exhibits the highest x_{Cl} and Y , which is in good accordance with the results in an early investigation on the immobilization of $AlCl_3$ using benzene and various chloroalkane solvents. In contrast, samples C1-3, C1-4, and C1-5 give very low x_{Cl} and Y . $AlCl_3$ and $TiCl_4$ can be immobilized on CDAC through strong bonding with oxygen groups or weak electrostatic interaction with the surface. In general, both interactions play changeable roles in helping activated carbon supports hold the guest active species. Meanwhile, the solvent can also have strong bonding interactions with $AlCl_3$ or $TiCl_4$. In the cases of diethyl ether and acetone with respect to catalysts C1-4 and C1-5, the coordination bonding interactions between $AlCl_3$ and solvent molecules become significant [36,37]. Specifically, diethyl ether (corresponding to catalyst C1-4) can chelate $AlCl_3$ and $TiCl_4$ to form stable complexes $AlCl_3 \cdot Et_2O$ and $TiCl_4 \cdot Et_2O$, respectively [38]. The interactions of active components with solvent molecules are stronger than those between active components and support, and therefore reduce the latter interactions. Consequently, the resulting catalysts have low x_{Cl} and Y . The C1-3 sample has a mediate content of active species but almost no activity for 1-decene oligomerization. This can be attributed to two reasons. First, alcoholysis can be involved in immobilization processes when using ethanol solvent. Also, $AlCl_3$ and ethanol can act as a Lewis acid and a Lewis base, respectively. As a result, the tin salt, which fails to catalyze the oligomerization

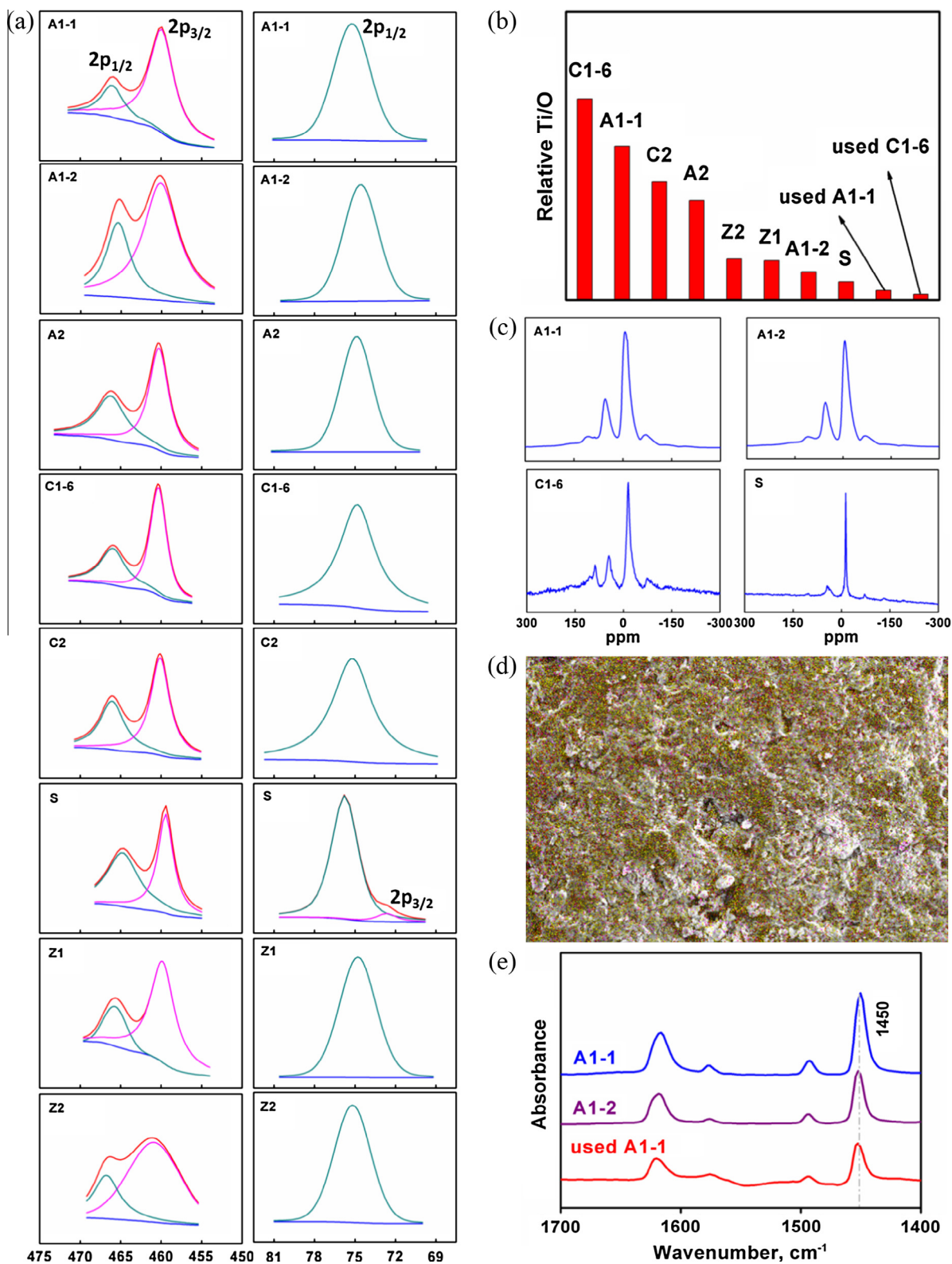


Fig. 3. Al/Ti dispersion and acidity measurement of catalysts: (a) XPS spectra, (b) relative Ti/O ratios on surfaces, (c) ^{27}Al MAS NMR spectra of A1-1, A1-2, C1-6 and S, (d) SEM/EDS map of sample A1-1 (red, yellow, and purple points represent Cl, Al, and Ti species, respectively), and (e) Py-IR spectra of A1-1, A1-2, and used A1-1 catalysts.

reaction, can be formed from the acid–base neutralization reaction and deposits onto the support. In contrast, carbon tetrachloride, benzene, and toluene, which have moderate solubility of AlCl_3 and TiCl_4 and weak active component–solvent interactions, impart high loading and catalytic activity to catalysts C1-1, C1-2, and C1-6.

3.3. Effect of immobilization time

The effect of reflux time on immobilization of AlCl_3 and TiCl_4 onto CDAC was also examined using carbon tetrachloride as solvent. The chlorine content of the supported catalysts initially increases with immobilization time and reaches a plateau at

13–14% with an immobilization time over 12 h (Fig. 2c). During immobilization, the aforementioned active species need to overcome the diffusion resistance to access to internal voids of supports and interact with internal surface sites. More immobilization time, therefore, is of rational benefit to loading of active species onto CDAC. However, the chlorine content no longer increases once the immobilization time is more than enough for a thermodynamic equilibrium state to be reached.

3.4. Effect of immobilization temperature

The corresponding results with respect to various catalysts prepared at different temperature for 12 h immobilization in carbon tetrachloride are presented in Table 3, indicating the considerable influence of temperature on the loading of active species as well as on the catalytic performance of the resulting catalysts. As temperature increases from 50 to 80 °C, x_{Cl} and Y increase from 9.8% to 14.2% and from 60.37% to 90.81%, respectively. Moreover, the viscosity of the PAO product also rises with increasing immobilization temperature. In addition to immobilization time, immobilization temperature can largely determine the diffusion rate of active species in both liquid solvent and porous support and thus affects the interaction between the active species and the support, which leads to distinct chlorine content and PAO yield. Furthermore, higher loading can provide higher catalytic activity for oligomerization of 1-decene, and therefore, the PAO product with a higher degree of oligomerization and a higher kinetic viscosity can be obtained (see Table 3). However, all oligomerization cases using different catalysts show comparable viscosity indices (in the range 154–161). This can be explained by the 1H NMR analysis results, which indicate that all PAO products have a very consistent branch ratio (the ratio of methyl to methylene groups in the oligomer [39]) of around 0.19.

3.5. Relationship of chlorine content (x_{Cl}) to yield of PAO (Y)

The chlorine content of supported catalysts prepared under various conditions was plotted against their corresponding yields of PAO products (see Fig. 2d). It is clearly shown that there is a linear relationship between x_{Cl} and Y , suggesting that the content of active species on the supported catalysts determines the catalytic oligomerization of 1-decene. However, the yields of PAO for catalysts C1-3, C1-4, and C1-5 deviate from this linear trend. It also can be ascribed to the strong interactions of active components with ethanol (for C1-3), diethyl ether (for C1-4), and acetone (for C1-5).

3.6. Stability of supported $AlCl_3$ - $TiCl_4$ catalysts

The lifetime test was carried out to evaluate the stability of supported catalysts. The oligomerization of 1-decene in a fixed-bed reactor filled with supported $AlCl_3$ - $TiCl_4$ catalysts was performed continuously. The yields of PAO with respect to different catalysts were plotted against time on stream (see Fig. 4). The catalytic activity of catalysts A1-1 and A2 displays very similar decreasing trends with increasing time on stream, suggesting the negligible

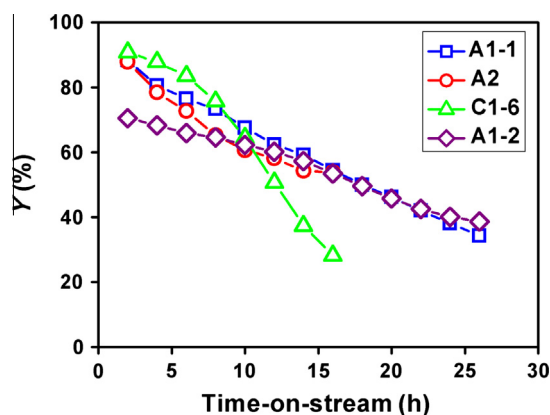


Fig. 4. The stability of different catalysts.

influence of pore size on catalytic stability. As compared with the three γ - Al_2O_3 -supported catalysts, C1-6 has higher initial activity, whereas it undergoes faster deactivation after 10 h, which indicates that γ - Al_2O_3 can provide supported catalysts with higher stability. In addition, a remarkable difference in initial activity and stability can be observed between catalysts A1-1 and A1-2. After 26 h, A1-1 and A1-2 still have yields of 34.3% and 38.7%, which account for 38.83% and 54.86% of their respective initial activity (88.36% for A1-1 and 70.54% for A1-2). $AlCl_3$ is located on the support in four forms: $(-Al-O)-AlCl_2$, $(-Al-O)_2-AlCl$, $(-Al-O)_3-Al$, and free $AlCl_3$ [30,40]. Correspondingly, $TiCl_4$ is also immobilized in both bonded and free forms [41,42]. As for the free active species, their nonbonding interaction with the support is weak. Considering the sublimation temperature of 178 °C for $AlCl_3$ and the boiling point of 136 °C for $TiCl_4$, heating postsynthesized catalysts accelerates the release of free active species from support, leading to low loading and therefore low initial catalytic activity. On the other hand, thermal treatment or high-temperature vapor deposition methods can benefit bonding between active species and support, which enhances the stability and life of catalysts [30,31,34].

3.7. Mechanism of deactivation of supported $AlCl_3$ - $TiCl_4$ catalysts

To figure out the deactivation mechanism of the supported catalysts, used samples were characterized carefully and compared with fresh ones. The SEM images for γ - Al_2O_3 support and fresh and used A1-1 catalysts are presented in Fig. 5a, b, and c. It is clearly shown that the support and fresh catalysts possess porous structures. Meanwhile, uniformly distributed active species can be observed on the surface of the fresh catalyst (see Fig. 5b). Results of N_2 adsorption (see Fig. 5d and e) indicate that the same fresh catalyst has a much smaller specific surface area (132.30 m^2/g) and larger average pore diameter (11.31 nm) than the parent support, which has a specific surface area of 281.38 m^2/g and an average pore diameter of 6.25 nm. Both the decrease of surface area and the increase of pore size are caused by partial pore blocking resulting from the immobilization of active species on the porous support. The morphology analysis also suggests the evolution in the pore structure of the deactivated catalyst. It seems that the porous structure almost disappears for the used catalyst sample (see Fig. 5c). Micropore analysis supports this view by providing a very small specific surface area of 29.95 m^2/g . In addition, the pore size distribution for the used catalyst shifts to larger values; as a result, the average pore diameter increases to 17.62 nm. Such changes in pore structure can be attributed to pore blockage and surface coverage. Oligomerization reactions can form oversized oligomer molecules that cannot diffuse out of the internal space through the size-limited channels of the catalyst, resulting in deactivation.

Table 3
Effect of immobilization temperature on chlorine content of supported catalyst and oligomerization.

Catalyst	T_1 (°C)	x_{Cl} (%)	Y (%)	v_{40} (mm ² /s)	v_{100} (mm ² /s)	VI
C1-12	50	9.8	60.37	44.51	8.125	158
C1-13	60	11.9	72.56	49.90	8.941	161
C1-14	70	13.1	81.05	54.60	9.324	154
C1-6	80	14.2	90.81	63.96	10.57	155

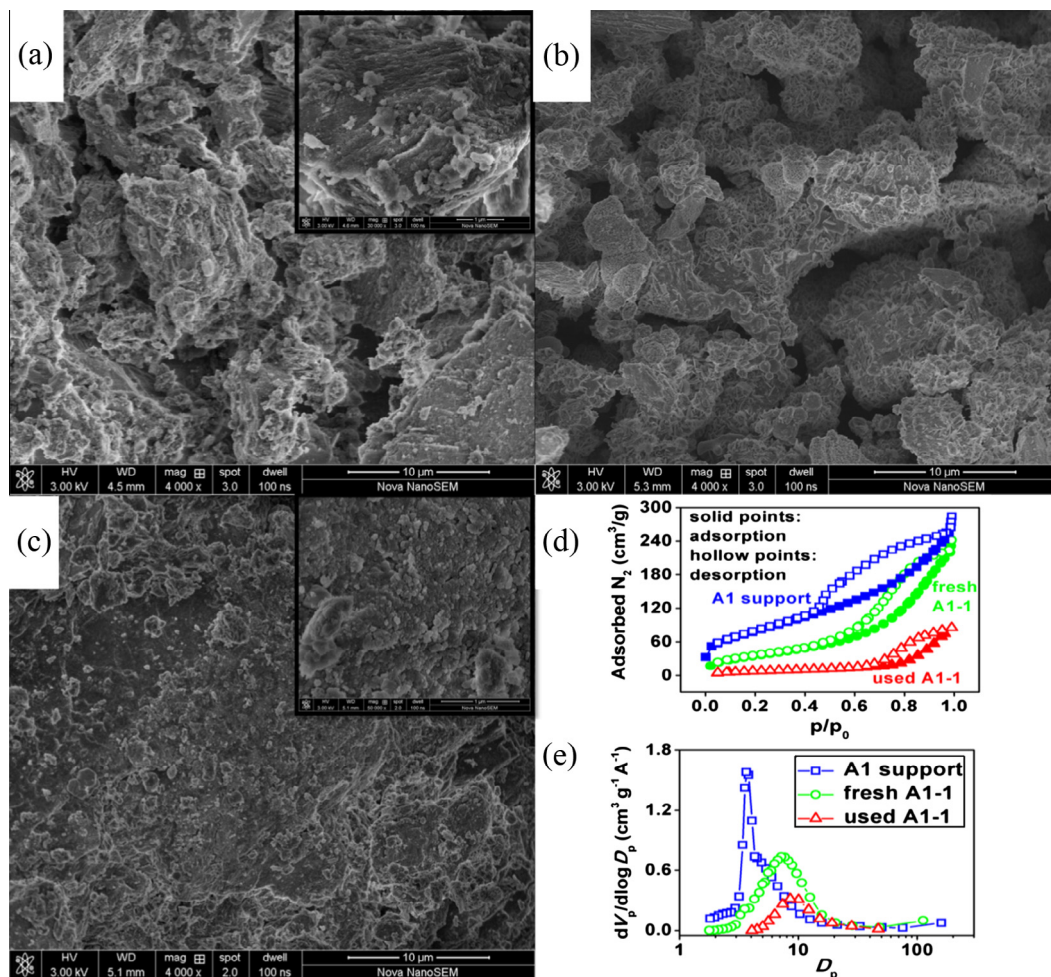


Fig. 5. SEM images of (a) support and (b) fresh and (c) used A1-1 catalysts (zoomed-in image shown in each top-right corner), (d) N_2 adsorption isotherm, and (e) pore size distribution.

In order to evaluate the content of oligomers trapped in the pores of the catalyst, TG–DSC analyses were carried out under oxygen flow. The used A1-1 has its main mass loss in the temperature range between 200 and 500 °C (accounting for 74.9% of total mass loss) and shows 6.52% higher overall mass loss than the corresponding fresh catalyst sample (Fig. 6a). When oxygen is during the TG–DSC analyses, both the mass loss with respect to over 300 °C in the TG trace (Fig. 6a) and the corresponding exothermic peaks (Fig. 6b) in the DSC curve denote the oxidation removal of the oligomers from the catalyst sample. For Fig. 6b, (used – fresh) A1-1 displays the corrected DSC signal of the used catalyst by subtracting a baseline, the signal of the fresh sample. Similar mass changes resulting from the oxidative removal of organic compounds have also been observed on heating coked zeolite 5A under oxygen flow [43].

In case of the γ - Al_2O_3 support, the mass decreases slowly on heating from room temperature to 800 °C. In the range from room temperature to 200 °C, the mass loss can be assigned to the dehydration of the support with an increase in temperature: hydroxyl water on the surface can be extracted. As for fresh catalyst A1-1, the mass loss was found to be 8.97% higher than that of A1 support. That can be attributed to the loss of active species. Furthermore, the DTA results support our aforementioned conclusion, that the catalyst A1-2 (with thermal treatment at 400 °C) has lower initial catalytic activity than A1-1 because of the release of free active species with heating. Reconsidering the sublimation temperature of $AlCl_3$ and boiling point of $TiCl_4$, fresh A1-1 undergoes

considerable mass decrease during heating, resulting from the escape of free active species. Moreover, a small part of the active species bonded with the support can be stripped at higher heating temperatures (i.e., higher than 600 °C). All of these results mean that the loss of active species should be considered to be an important aspect to explain the deactivation mechanism of supported $AlCl_3$ – $TiCl_4$ catalyst.

The elemental analyses for fresh and used catalysts were done to confirm the changes in active species content of supported catalysts during the oligomerization process. For the sake of comparison between fresh and used catalyst, the atomic fraction of oxygen was selected as the reference. The EDS results (see Fig. 6c) agree with our previous analysis very well. The atom ratios C/O, Al/O, and Ti/O are found to be 0.247, 0.698, and 0.130 for fresh A1-1 and 1.423, 0.585, and 0.020 for used A1-1, respectively. The deactivated catalyst has a higher C/O ratio because of the deposition of oligomer compounds, and lower Al/O and Ti/O ratios owing to the loss of active species. Ti/O for the surface of used A1-1 derived from XPS analysis can also agree with that by displaying a lower value than for the fresh catalyst (Fig. 3b). Consequently, the acidity of the deactivated catalyst is greatly reduced (Fig. 3e), and thus provides decreasing catalytic activity.

Chlorine content of used catalysts was determined and illustrated in Fig. 6d. The chlorine content in synthesized PAO products was also analyzed. As it can be seen, both chlorine contents exhibit damped decrease with increasing time on stream. In addition, the content of Al and Ti in the PAO product collected in the initial

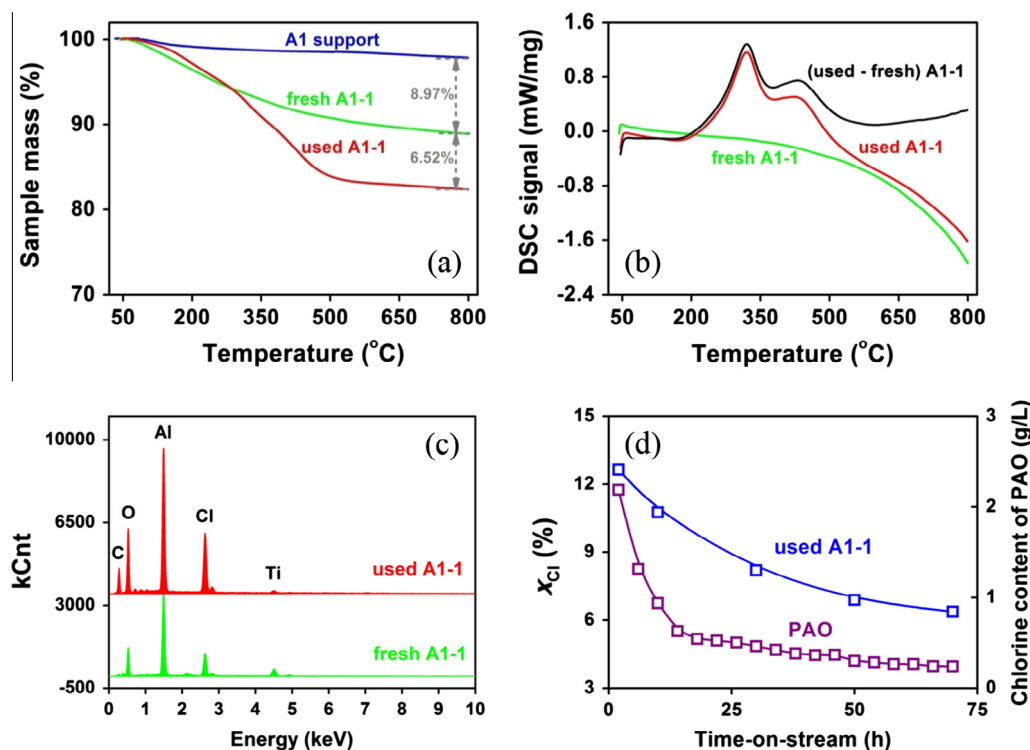


Fig. 6. Characterization of catalysts and PAO products: (a) TG and (b) DSC curves for support and fresh and used A1-1 catalysts, (c) EDS analysis profiles for fresh and used A1-1 catalysts, and (d) chlorine content of A1-1 catalyst and PAO during oligomerization.

reaction stage were measured. The observed concentrations of Al and Ti are 1100 and 320 mg/L, respectively. Such results clearly indicate active species transfer from catalyst bulk to liquid stream.

The loss of active species is also confirmed to be the main reason for the deactivation of CDAC-supported catalyst. From our ICP analysis results, the content of Al, Ti, and Cl species contained in the product stream is around 600, 193, and 2810 mg/L at 6 h time on stream. It was also supported by our SEM/EDS analysis (results not given).

To sum up, all results presented here lead to the conclusion that the deactivation of supported catalysts results from two main aspects: the blockage and coverage of the pore structure of the support by deposited oligomers, and the loss of active species during the oligomerization process. The decreasing number of active sites and increasing diffusion resistance jointly cause the supported catalyst to lose catalytic activity, resulting in a declining yield of PAO product.

4. Conclusions

Oligomerization of 1-decene was studied in a fixed-bed reactor with a series of Al-Ti bimetallic catalysts prepared by anchoring AlCl_3 and TiCl_4 onto different supports under varying preparation conditions. The active species are highly dispersed on the surfaces of the supports. Their catalytic activities and stabilities were evaluated and the deactivation mechanism was revealed in terms of catalyst characterizations and active species determination. There is a linear relationship between PAO yield and chlorine content of supported catalysts. For CDAC-supported catalyst, the highest chlorine content and PAO yield are found to be 14.2% and 90.81%, respectively. However, $\gamma\text{-Al}_2\text{O}_3$ enables the supported catalyst to achieve a higher stability than others. Deactivation of supported catalysts can be attributed mainly to the blockage and

coverage of the pore structure by deposited oligomers and the loss of active species.

Acknowledgments

This work was financially supported by the National Natural Science Foundation of China (21201063), the Natural Science Foundation of Shanghai, China (16ZR1408100) and the Specialized Research Foundation for the Doctoral Program of Higher Education of China (20110074120020).

References

- [1] J.A. Brennan, Wide-temperature range synthetic hydrocarbons fluids, *Ind. Eng. Chem. Prod. Res. Dev.* 19 (1980) 2–6.
- [2] G.R. Lappin, J.D. Sauer, *Alpha Olefin Application Handbook*, Marcel Dekker, New York, 1989.
- [3] L.R. Rudnick, R.L. Shubkin, *Synthetic Lubricants and High-performance Functional Fluids*, Marcel Dekker, New York, 1999.
- [4] W.R. Murphy, D.A. Blain, A.S. Galiano-Roth, P.A. Galvin, Benefits of synthetic lubricants in industrial applications, *J. Synth. Lubr.* 18 (2002) 301–325.
- [5] S. Boyde, Green lubricants. Environmental benefits and impacts of lubrication, *Green Chem.* 4 (2002) 293–307.
- [6] G.D. Yadav, N.S. Doshi, Development of a green process for poly-alpha-olefin based lubricants, *Green Chem.* 4 (2002) 528–540.
- [7] S.A. Culley, M.T. Devlin, J. McAllister, A.J. Rollin, R. Iyer, H. Maelger, Reduction in CO_2 emissions by optimization of transmission fluids for improved vehicle fuel economy, in: *Proceedings of the International Joint Tribology Conference*, Hiroshima, Japan, 2011.
- [8] V.C. Gibson, S.K. Spitzmesser, Advances in non-metallocene olefin polymerization catalysis, *Chem. Rev.* 103 (2003) 283–315.
- [9] A. Kermagoret, P. Braunstein, SHOP-type nickel complexes with alkyl substituents on phosphorus, synthesis and catalytic ethylene oligomerization, *Dalton Trans.* (2008) 822–831.
- [10] C. Bianchini, G. Giambastiani, L. Luconi, A. Meli, Olefin oligomerization, homopolymerization and copolymerization by late transition metals supported by (imino)pyridine ligands, *Coord. Chem. Rev.* 254 (2010) 431–455.
- [11] D.S. McGuinness, Olefin oligomerization via metallacycles: dimerization, trimerization, tetramerization, and beyond, *Chem. Rev.* 111 (2011) 2321–2341.
- [12] K.H. Theopold, Homogeneous chromium catalysts for olefin polymerization, *Eur. J. Inorg. Chem.* (1998) 15–24.

- [13] H. Zhang, J.L. Huang, Y.L. Qian, Progress in synthesis of homogeneous chromium catalysts and their application in olefin polymerization, *Chin. J. Org. Chem.* 22 (2002) 981–989.
- [14] P. Wasserscheid, S. Grimm, R.D. Kohn, M. Haufe, Synthesis of synthetic lubricants by trimerization of 1-decene and 1-dodecene with homogeneous chromium catalysts, *Adv. Synth. Catal.* 343 (2001) 814–818.
- [15] H. Sinn, W. Kaminsky, H.J. Vollmer, R. Woldt, Living polymers' with Ziegler catalysts of high productivity, *Angew. Chem.* 92 (1980) 396–402.
- [16] H.G. Alt, A. Koppl, Effect of the nature of metallocene complexes of group IV metals on their performance in catalytic ethylene and propylene polymerization, *Chem. Rev.* 100 (2000) 1205–1221.
- [17] G.W. Coates, Precise control of polyolefin stereochemistry using single-site metal catalysts, *Chem. Rev.* 100 (2000) 1223–1252.
- [18] J. Gromada, J.F. Carpentier, A. Mortreux, Group 3 metal catalysts for ethylene and alpha-olefin polymerization, *Coord. Chem. Rev.* 248 (2004) 397–410.
- [19] T. Akio, H. Suzuka, Boron phosphate as a highly active catalyst for 1-decene oligomerization, *Chem. Lett.* 16 (1987) 423–424.
- [20] R.S. Drago, E.E. Getty, Preparation and catalytic activity of a new solid acid catalyst, *J. Am. Chem. Soc.* 110 (1988) 3311–3312.
- [21] A. de Klerk, Oligomerization of 1-hexene and 1-octene over solid acid catalysts, *Ind. Eng. Chem. Res.* 44 (2005) 3887–3893.
- [22] C.S.H. Chen, R.F. Bridger, Shape-selective oligomerization of alkenes to near-linear hydrocarbons by zeolite catalysis, *J. Catal.* 161 (1996) 687–693.
- [23] R. Van Grieken, J.M. Escola, J. Moreno, R. Rodriguez, Liquid phase oligomerization of 1-hexene over different mesoporous aluminosilicates (Al-MTS, Al-MCM-41 and Al-SBA-15) and micrometer/nanometer HZSM-5 zeolites, *Appl. Catal., A: Gen.* 305 (2006) 176–188.
- [24] M. Cadenas, R. Bringue, C. Fite, E. Ramirez, F. Cunill, Liquid-phase oligomerization of 1-hexene catalyzed by macroporous ion-exchange resins, *Top. Catal.* 54 (2011) 998–1008.
- [25] R. Bringue, M. Cadenas, C. Fite, M. Iborra, F. Cunill, Study of the oligomerization of 1-octene catalyzed by macroreticular ion-exchange resins, *Chem. Eng. J.* 207 (2012) 226–234.
- [26] A. Finiels, F. Fajula, V. Hulea, Nickel-based solid catalysts for ethylene oligomerization – a review, *Catal. Sci. Technol.* 4 (2014) 2412–2426.
- [27] A.P. Wight, M.E. Davis, Design and preparation of organic–inorganic hybrid catalysts, *Chem. Rev.* 102 (2002) 3589–3613.
- [28] C. del Pozo, A. Corma, M. Iglesias, F. Sanchez, Immobilization of (NHC)NN-pincer complexes on mesoporous MCM-41 support, *Organometallics* 29 (2010) 4491–4498.
- [29] A. Kermagoret, R.N. Kerber, M.P. Conley, E. Callens, P. Florian, D. Massiot, F. Delbecq, X. Rozanska, C. Coperet, P. Sautet, Chlorodiethylaluminum supported on silica: a dinuclear aluminum surface species with bridging $\mu(2)$ -Cl-ligand as a highly efficient co-catalyst for the Ni-catalyzed dimerization of ethene, *J. Catal.* 313 (2014) 46–54.
- [30] A. Krzywicki, M. Marczewski, Superacidity of modified γ -Al₂O₃. Structure of active site and catalytic activity, *J. Chem. Soc., Faraday Trans. 1* 76 (1980) 1311–1322.
- [31] S. Sato, G.E. Maciel, Structures of aluminum chloride grafted on silica surface, *J. Mol. Catal. A: Chem.* 101 (1995) 153–161.
- [32] D. Dube, S. Royer, D.T. On, F. Beland, S. Kaliaguine, Aluminum chloride grafted mesoporous molecular sieves as alkylation catalysts, *Microporous Mesoporous Mater.* 79 (2005) 137–144.
- [33] T. Xu, N. Kob, R.S. Drago, J.B. Nicholas, J.F. Haw, A solid acid catalyst at the threshold of superacid strength-NMR, calorimetry, and density functional theory studies of silica-supported aluminum chloride, *J. Am. Chem. Soc.* 119 (1997) 12231–12239.
- [34] T.X. Cai, M. He, New approaches to immobilization of aluminum chloride on gamma-alumina and its regeneration after deactivation, *Catal. Lett.* 86 (2003) 17–23.
- [35] L. Wang, C. Cai, Polystyrene-supported AlCl₃: a highly active and reusable heterogeneous catalyst for the one-pot synthesis of dihydropyrimidiones, *J. Heterocyclic Chem.* 45 (2008) 1771–1774.
- [36] A. Samadi-Maybodi, S.M. Pourali, M. Tafazzoli, Aluminum solvate complexes forming in acidic methanol-acetone mixtures studied by Al-27 NMR spectroscopy, *J. Solution Chem.* 38 (2009) 159–169.
- [37] G.T. Castro, S.E. Blanco, S.L. Arce, F.H. Ferretti, Characterization and structural study of the complex of Al(III) with 2,4-dihydroxy-benzophenone. Ionic strength and solvent effects, *Spectrochim. Acta A* 59 (2003) 2685–2696.
- [38] G.L. Guo, Y.C. Xie, Y.Q. Tang, Effect of titanium ether complex on the surface structure of the 3TiCl₃-AlCl₃ catalyst, *Acta Phys.-Chem. Sin.* 1 (1982) 57–65.
- [39] Q.G. Huang, L.G. Chen, Y.P. Sheng, L. Ma, Z.F. Fu, W.T. Yang, Synthesis and characterization of oligomer from 1-decene catalyzed by AlCl₃/TiCl₄/SiO₂/Et₂AlCl, *J. Appl. Polym. Sci.* 101 (2006) 584–590.
- [40] V.R. Choudhary, K. Mantri, AlCl₃-grafted Si-MCM-41: influence of thermal treatment conditions on surface properties and incorporation of Al in the structure of MCM-41, *J. Catal.* 205 (2002) 221–225.
- [41] L. Lu, H. Niu, J.Y. Dong, Propylene polymerization over MgCl₂-supported TiCl₄ catalysts bearing different amounts of a diether internal electron donor: extrapolation to the role of internal electron donor on active site, *J. Appl. Polym. Sci.* 124 (2012) 1265–1270.
- [42] S.S. Haukka, E.L. Lakomaa, A. Root, An IR and NMR study of the chemisorption of titanium tetrachloride on silica, *J. Phys. Chem.* 97 (1993) 5085–5094.
- [43] H. Sun, B.X. Shen, Experimental study on coking, deactivation, and regeneration of binderless 5 Å zeolite during 1-hexene adsorption, *Adsorption* 19 (2013) 111–120.